CRYSTALLOGRAPHIC FEATURES OF MECHANICALLY MILLED AND ALLOYED NANOSIZED CRYSTALLINE AND AMORPHOUS MATERIALS †

Antun Tonejc
Faculty of Science, Department of Physics, Bijenička 32, 10002 Zagreb, Croatia;
e-mail:atonejc@phy.hr

† Plenary lecture held at the 9th Slovenian-Croatian Meeting, Gozd-Martuljek, Slovenia, June 15-17, 2000.

Received 01-06-2001

Abstract

High energy mechanical ball milling, which includes mechanical alloying (MA) and mechanical grinding (MG), has been extensively used in the last 20 years as a non-equilibrium processing method analogous to the previous interest in very rapid solidification cooling (rates from 10^6 to 10^{10} K/s) for synthesizing, at room temperature, all kinds of materials.

Both mechanical alloying of dissimilar powders and mechanical grinding of single composition powder have resulted in a wide variety of entirely new metastable alloys including amorphous alloys, nanocrystalline materials, extended solid solutions, alloys from elements with a widely different melting point, all sorts of compounds and composites and otherwise difficult to process novel materials, and even those alloys which are immiscible by conventional processing methods.

The crystallite size of MA and MG materials decreases rapidly with milling time to reach a saturation value, generally in the range from 1 to 30 nm, attributing the name nano-sized materials to MA and MG end products.

During the milling process the interaction between milling balls and powder particles can be characterized by processes like cold-welding, plastic deformation and further fragmentation of the particles. A high defect structure of the lattice, the immense magnification of the boundary surface and high diffusion rate leads to low activation energies for the transformation of the structure.

The current state of the mechanism of the metastable phase formation during milling in systems which exhibit a negative heat of mixing of the components will be given from the thermodynamic and kinetic viewpoints. On the other hand, although phase formation in systems with positive heats of mixing is far from being understood, a possible explanation will also be given.

Various application areas where the MA technology could be used will be illustrated as well.

1. Introduction

In 1960 P. Duwez have invented a non-equilibrium processing techniques, called ultra-rapid quenching (URQ) technique, in which the melt could be cooled to room temperature by quenching rates more than 10^6 K/s.[1] The results have shown that this novel processing enables to increase defect concentrations, to achieve microstructural refinement, to produce supersaturated solid solutions with solute levels

far beyond the equilibrium limit at any temperature, metastable phases and even the amorphous structure in many systems (called metallic glasses in the case of alloys). Since then this technique has since been used in many laboratories for fundamental studies and has been adopted as an important commercial production process, particularly for magnetic materials.[2] However in the mid of 1980s interest turned also to solid-state processing which in fact started in 1970 with the J. S. Benjamin's article[3] in which he described a new processing technique, called mechanical alloying (MA) and was based on high energy ball milling. His aim was to combine fine particle dispersion strengthening with age hardening in a nickel-base superalloy for high-temperature applications. He found out that the end product possessed better high-temperature dispersion strengthening than the superalloys of the same composition prepared by more conventional methods. He also suggested that this technique be otherwise applicable also to the preparation of metastable structure. Although J. S. Benjamin in his articles gave the technical details of high energy ball milling procedure and even proposed the model of mechanical alloying, it is very curious that his work was largely disregarded for more then a decade.

In 1979 R. L. White was the first who reported the preparation of amorphous Nb_3Sn alloy from elemental niobium and tin powder[4] by high-energy ball milling, and in 1981 A. E. Yermakov and al.[5] reported the producing of amorphous powders of Y-Co alloys by milling Y-Co compounds in a ball mill on the basis of X-ray diffraction pattern which showed typical broad peak, characteristic of amorphous material. The two works have not attracted the attention till the next two papers appeared, by C. C. Koch and al. in 1983[6] and by R. B. Schwarz in 1985.[7] The first paper reported on the formation of amorphous $Ni_{60}Nb_{40}$ alloy from elemental nickel and niobium powders using MA procedure. In the second paper, it was reported that both extended solid solutions and amorphous alloys over broad composition ranges (Ni_xTi_{1-x}) were produced by MA of elemental nickel and titanium powders showing that the range of amorphization was broader than in samples prepared by URQ from the melt.

In the years which followed the number of published papers grew gradually from about 50 papers in 1986 to about 500 papers in 1992. At present about 3 to 4 papers are published per day on the subject.

2. Experimental

During the last three decades various types of high-energy mills have been used for milling, including planetary mill, attrition mill and vibratory mill (Fig. 1).[8,9]

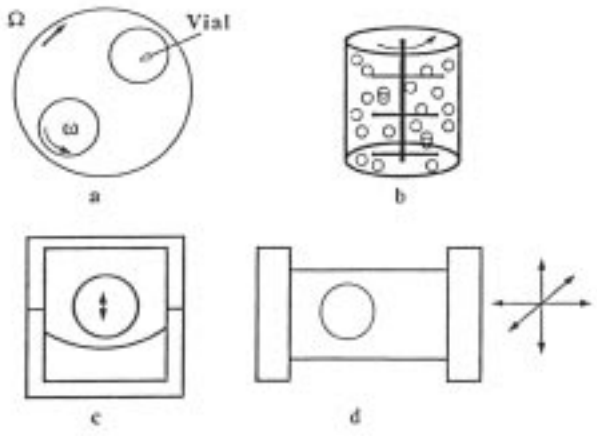

Figure 1. Various types of mills: (a) planetary mill; (b) attrition mill; (c) and (d) vibratory mills.

Planetary mills are the most widely used in laboratories. They have three important parts: rotating disc, containers/vials and balls. A rotating disc bears vials (two or four, of about 6 cm in diameter), with balls inside the vial. The disc and the vials rotate in the opposite direction. The rotation speeds (Ω and ω) which are of the order of several hundred rpm could be varied independently. During the rotation there is a lot of impact between the balls and the balls and the vial. The impact speed of the balls is of the order of several ms^{-2} and shock frequencies are several hundred Hz. Balls and vials are usually made of hardened steel and tungsten carbide (WC+6wt%Co), but material like zirconia, alumina (corundum), agate, copper, Cu-Be alloy, etc. are also used. Powders of the material to be milled are introduced in the required proportions into the vial together with the balls.

In order to avoid oxidation the vials are often sealed under purified argon inside a glove box. Even the powders to be milled are also weighed and mixed in this glove box, so that the total handling of the powders and the milling are carried out under protective

atmosphere. Argon is the most used atmosphere, while when using nitrogen or hydrogen atmosphere nitrides or hydrides appeared. Milling under vacuum, in helium atmosphere or in air is also often the case.

For X-ray diffraction (XRD) measurements or transmission electron microscopy (TEM) investigations the milling is interrupted at selected times to remove the powder, and then put back into the vial for further milling. For the examination of physical properties for which bulk samples are needed the powders are sintered, hot comprised, hot extruded or shock way compacted.

Typical milling condition values are: the ball-to-powder weight ratio from 3:1 to 30:1, the total mass of powders 0.5 to 15 g, starting particle size from 45 to 150 μm, a set of 10 balls of 10 mm in diameter and 4 balls of 12 mm in diameter. However, after some trial and error tests each researcher usually determines the best milling conditions. Also, depending on the starting conditions of the material to be milled, it exists two possible kinds of milling: a) mechanical alloying (MA), if the starting material consists of a mixture of pure elemental powders; b) mechanical grinding (MG), if the starting material consists of a compound previously synthesized. The expression mechanical milling (MM) includes both methods.

3. Some important experimental facts

3.1. Nanosized materials

C. C. Koch and al., in his paper published in 1983,[6] already observed a decrease of the "effective crystallite/grain" size (calculation done by using the Scherrer formula $L=0.9\lambda/(\beta \cos \theta)$) down to nano-dimensions during the milling and finally to the value which corresponds to the width of the peak of the eventually obtained amorphous alloy (Fig. 2). In the early stages of milling the grain size decreases rapidly to reach a steady state after prolonged milling, and shows to be composition dependent (Fig. 3),[10] to vary from element to element (Fig. 4),[10] and decreases in size below 10 nm for elements with high melting temperatures (Fig. 5).[11] The decrease of the grain size to nano-size dimension has become a common feature of the mechanically milling process (Fig. 6(a-d)).[12]

The reduction of crystallite size due to milling down to nanometer-sizes which has been observed at the very beginning of the milling experiments coincided with H. Gleiter's idea in 1980[13,14] who pointed out that polycrystals in which the size of individual crystallites is of the order of several (1-10) nanometers (Fig. 7) consist of two

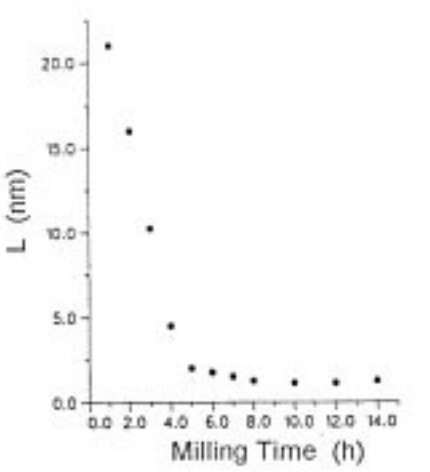

Figure 2. Average crystallite size vs milling time in the Ni-Nb powder during the MA in air.[6]

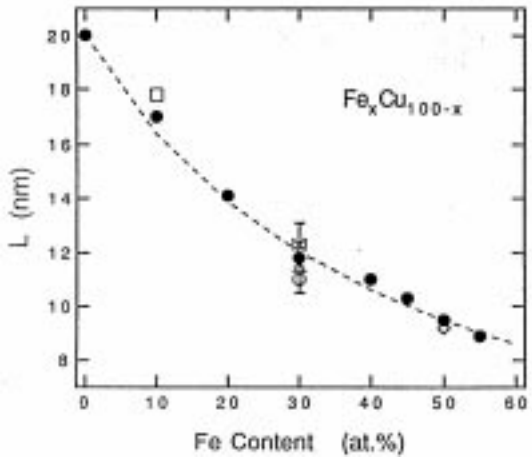

Figure 3. Average crystallite size obtained by MA for Fe_xCu_{10-x} powders after 24 h of milling vs Fe content.[10]

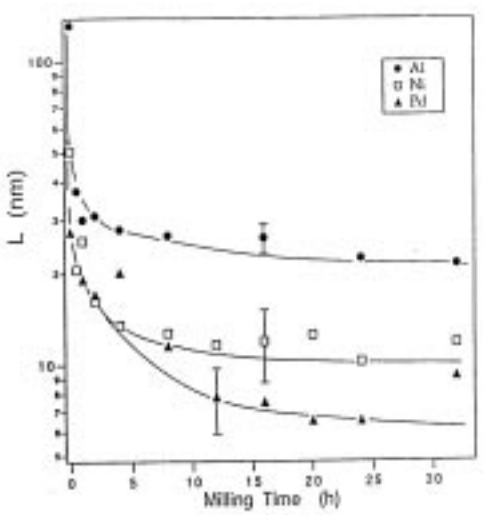

Figure 4. Average crystallite size of Al, Ni, and Pd vs ball milling time.[10]

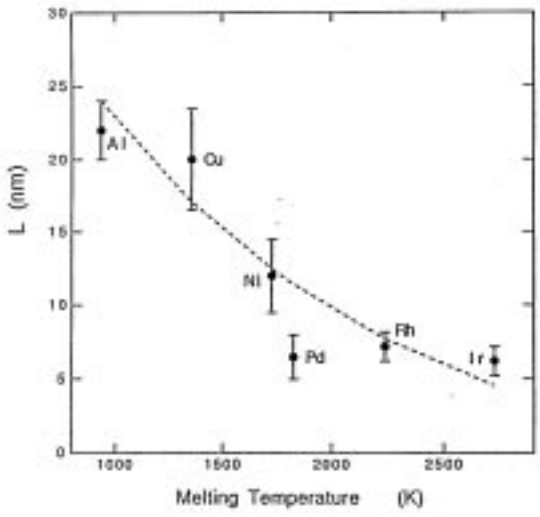

Figure 5. Minimum crystallite size obtained by ball milling for different fcc metals vs melting temperatures.[11]

components: a crystallite component formed by all atoms located in the lattice of the crystallites, and an interfacial component comprising all atoms which are situated in the crystallite (or interphase) boundary between the crystallites. Such a material consisting

of a large fraction of incoherent interfaces should deviate significantly in structure and properties from those crystalline and/or glass materials of the same composition. The prediction was confirmed during the next years (e.g. References 9,13,15, and Fig. 8).

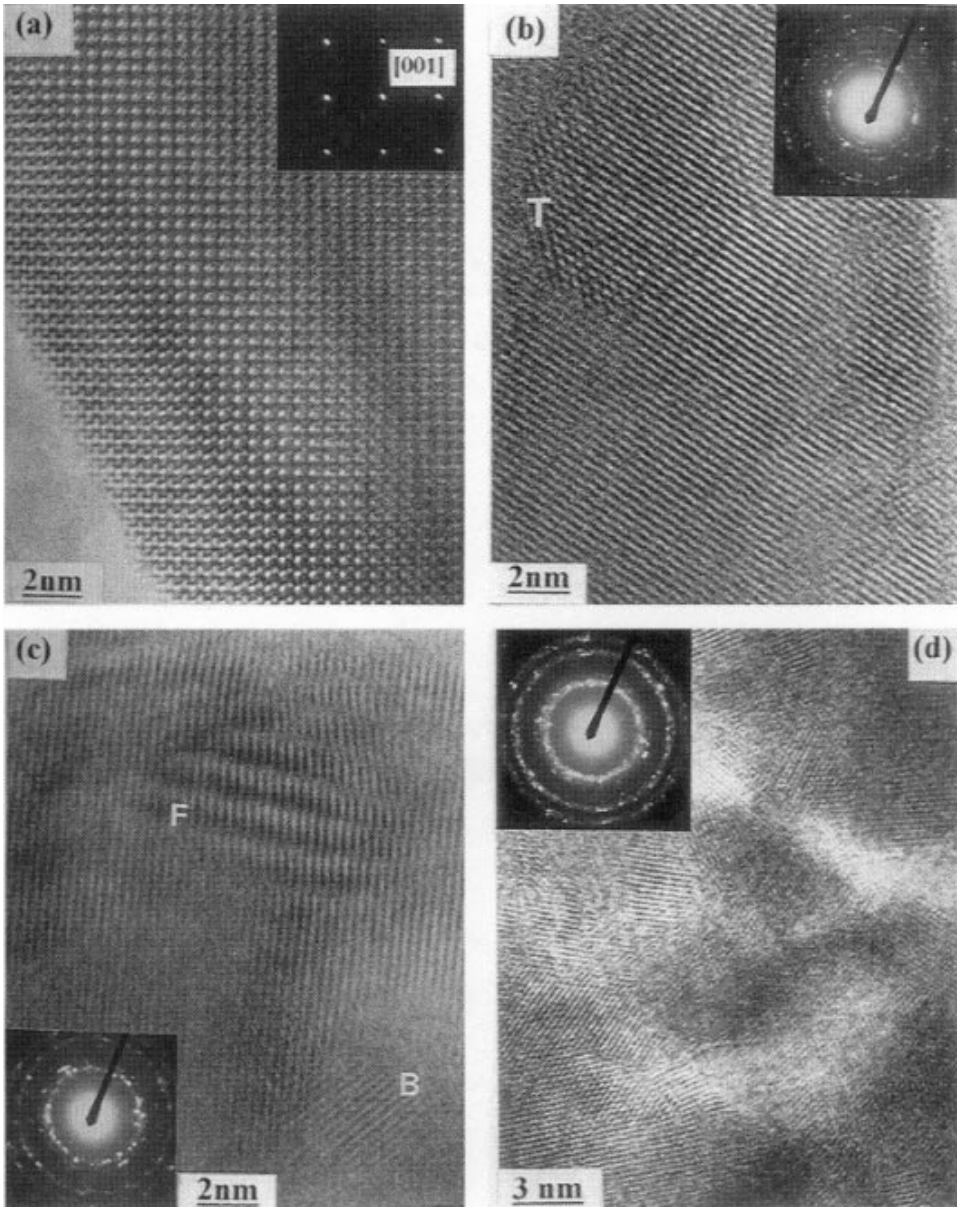

Figure 6. HRTEM lattice image of: (a) monoclinic ZrO_2 viewed along [001] direction (crystallite size is 200 nm); (b) d_{111} lattice image of a sample of the 2.5 g ZrO_2 and 0.5 g Y_2O_3 powder mixture milled for 10 minutes. Tetragonal crystallite T is stuck on large monoclinic ZrO_2 oxide grain having layered structure, deformed and ruptured lattice planes; (c) a sample of the 2.5 g ZrO_2 and 0.5 g Y_2O_3 powder mixture milled for 1 h. Stacking faults or antiphase boundary f and crystallite b stuck on larger crystallite; (d) a sample of the 2.5 g ZrO_2 and 0.5 g Y_2O_3 powder mixture milled for 3 h. Crystallite sizes from 2 to 12 nm. Corresponding SAD patterns are shown as the inserts.[12]

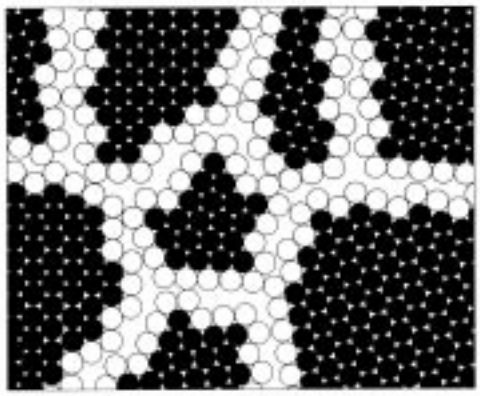

Figure 7. Two-dimensional hard sphere model of the atomic structure of a nanocrystalline material. For clarity the atoms in the boundary core regions are presented by open circles.[13]

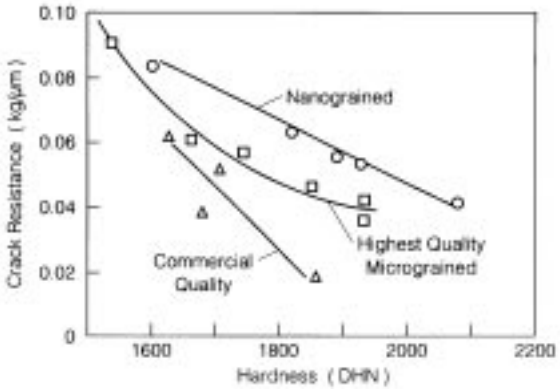

Figure 8. Comparison of the crack resistance of hardness of nano-crystalline and commercial grades of fully sintered WC-Co materials.[13]

Estimation showed[13] that if the crystallite size is of the order of 5 to 10 nm, about 50% of the atoms should be located in interfaces forming the interfacial component without long- (characteristic of the crystalline component) or short-range order (characteristic of the amorphous/glassy component).[13] For that reason such materials could not be classified neither as really crystalline materials nor as glassy materials. They comprise something like a new "third solid state structure" and H. Gleiter called such materials nanocrystalline materials. We can state that starting with Gleiter's definition of nanocrystalline materials both subject "mechanically milling" and "nanocrystalline materials" are interconnected and have developed side by side. Depending on particular subjects numerous expressions started to be used in the literature, like: nanocrystals, nanocrystalline materials, nanophase materials, ultrafine grain sized materials, ultrafine microstructure, nanostructured materials, nonometer sized materials, nanoamorphous material, nanoglasses, submicron glasses. We think that the expression "nanosized materials" covers all these terms and should be used as the general expression.

3.2. Equivalence of the mechanical alloying (MA) and

of the mechanical grinding (MG)

Amorphous alloys can be formed by mechanical alloying (MA) when the starting powders are a mixture of pure metal powders or by mechanical grinding (MG) when the starting material is a crystalline intermetallic synthesized previously. The comparison of the results showed that although the amorphization by MA and MG seemed to occur by different mechanisms, the diffraction patterns are almost identical in both cases (Fig. 9), but the required processing time for a fully amorphous product is approximately half the period as when the elements were the starting material.[16-18]

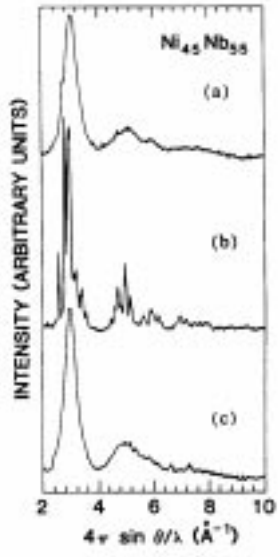

Figure 9: (a) amorphous $Ni_{45}Nb_{55}$ obtained after MA pure crystalline Ni and Nb powders for 11h; (b) crystalline $Ni_{45}Nb_{55}$ powder prepared by crushing an arc melting ingot of the intermetallic; (c) amorphous $Ni_{45}Nb_{55}$ powder obtained by MG powder in curve (b) for 14 h.[16]

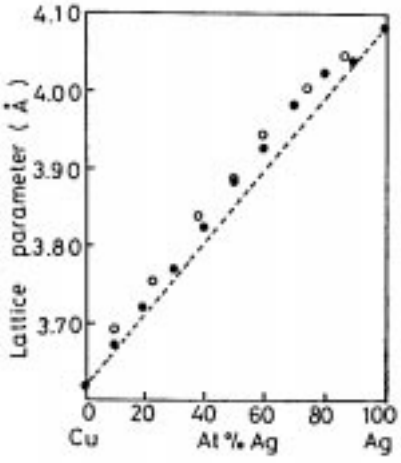

Figure 10. Lattice parameter of the Ag-Cu alloys produced by MA (•) and by ultra rapid quenching (o).[19]

3.3. Equivalence of ultra-rapid quenching and mechanical alloying/grinding

After P. Duwez published his paper in 1960,[1] ultra-rapid quenching has been the most widely used method for producing non-equilibrium phases till the invention of mechanical milling procedure, and it is not surprising that the researches were attracted to the idea if the MA and URQ methods give the same end products.

One of many spectacular achievements of the URQ method was the creation of a supersaturated Ag-Cu fcc solid solution on the entire composition range, although silver

and copper are almost immiscible to each other. The complete metastable solubility was also obtained by MA (Fig. 10),[19] which proved that MA is just as effective as URQ in producing a complete solid solution in the Ag-Cu system.

Iron and copper, which exhibit vanishing small mutual solid solubility under the equilibrium conditions, form supersaturated solid solutions up to 20at.%Fe in Cu (15at.%Cu in Fe) when solidified by URQ,[20] but even up to 60at.%Fe (15at.%Cu in Fe) using MA.[21]

In the X-ray diffraction pattern of the rapidly quenched sample, if compared with that of the MA powder sample (e.g. the case of $Ti_{57}Cu_{43}$ alloy[22]), it was found out that the two diffraction patterns have quite similar characteristics (Fig. 11), and that the composition dependence of the nearest-neighbor distance in amorphous samples obtained by URQ, MA and by vapor quenching showed good agreement between data (Fig. 12).[18]

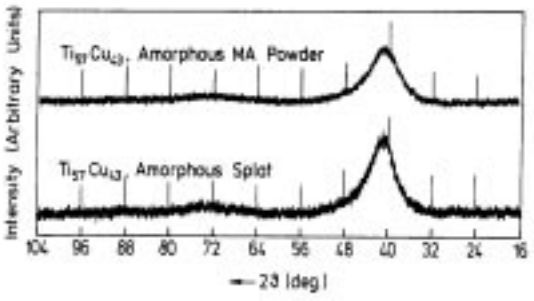

Figure 11. Comparison of X-ray diffractograms of amorphous $Ti_{57}Cu_{43}$ MA powder (mechanically alloyed 6 h) with amorphous $Ti_{57}Cu_{43}$ prepared by ultra rapid quenching.[22]

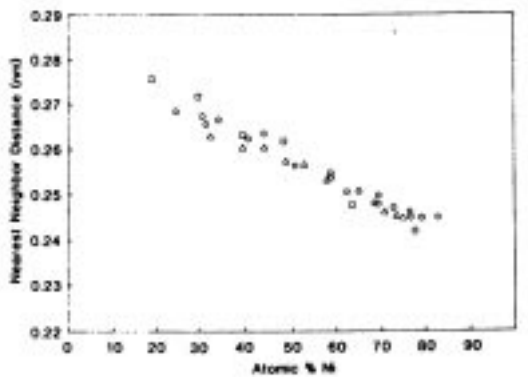

Figure 12. Nearest neighbor distance of amorphous Ni-Nb prepared by MA (squares), vapour quenching (circles) and ultra rapid quenching.[18]

The simple cubic structure with one atom per cell is rare in crystalline solids, and α-Po is the only known element found to exhibit this structure under equilibrium conditions. By applying the URQ technique, it is possible to produce the metastable simple cubic phase in Ag-Te alloy. However, the extent to which the simple cubic phase forms on milling is restricted compared to rapid solidification.[23]

The system Cu-Nb-Sn is an example where an amorphous phase can be formed by MA but not by rapid quenching,[24] or the glass-forming range is not the same for URQ

and MA as in the Fe-Zr system (Fig. 13).[25, 26] Whereas URQ produces amorphous alloy preferentially close to deep eutectics, in MA process amorphous alloys are formed in the central part of the phase diagram, i.e. also in the range of high melting point intermetallic phases.

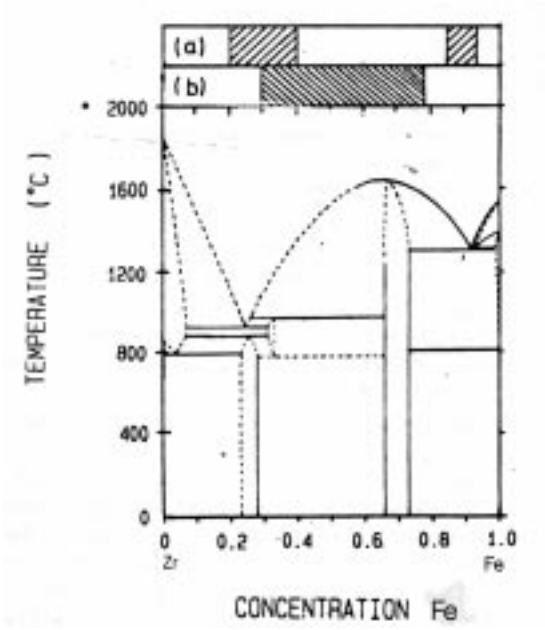

Figure 13. Phase diagram of the Fe-Zr system including the glass-forming ranges of (a) ultra rapid quenching and (b) mechanically alloyed samples.[26]

As a conclusion it can be stated that amorphous alloys obtained in both processes, URQ and MA, are structurally very similar (the position of the maximum in the diffraction pattern is independent of the preparation technique), both topologically and chemically, and that the MA is a more efficient method than URQ in the formation of the non-equilibrium phases like amorphous alloys and supersaturated solid solutions. The only difference was found in the value of the crystallization temperature of the amorphous alloys which showed to be higher for samples prepared by milling than that of the URQ samples.[18]

3.4. Nanoamorphous materials are they really amorphous?

When using the Scherrer equation it is generally accepted that if the halo peak corresponds to the "apparent" crystallite size lower than 2.0 nm, it should be used as an indication of an amorphous state. This condition is fulfilled in MA alloys. It is also

known that the superconducting transition temperature and the crystallization temperature in pure amorphous structure are composition dependent and being constant in the two phase (amorphous and crystalline) region, which has been confirmed in a number of binary alloys proving that mechanically alloyed powders become amorphous during milling.[25, 26]

3.5. Equivalence of mechanical milling and thermal treatment

It is well known that heating of boehmite or gibbsite at over 1000^0C yields a variety of transition aluminas before the stable corundum is formed:

$$\underset{\text{boehmite}}{} \xrightarrow{>350^0\text{C}} \gamma\text{-}Al_2O_3 \xrightarrow{>700^0\text{C}} \delta\text{-}Al_2O_3 \xrightarrow{>900^0\text{C}} \theta\text{-}Al_2O_3 \xrightarrow{>1000^0\text{C}} \alpha\text{-}Al_2O_3$$

$$\underset{\text{gibbsite}}{} \xrightarrow{>170^0\text{C}} \chi Al_2O_3 \xrightarrow{>600^0\text{C}} \kappa\text{-}Al_2O_3 \xrightarrow{>850^0\text{C}} \alpha\text{-}Al_2O_3$$

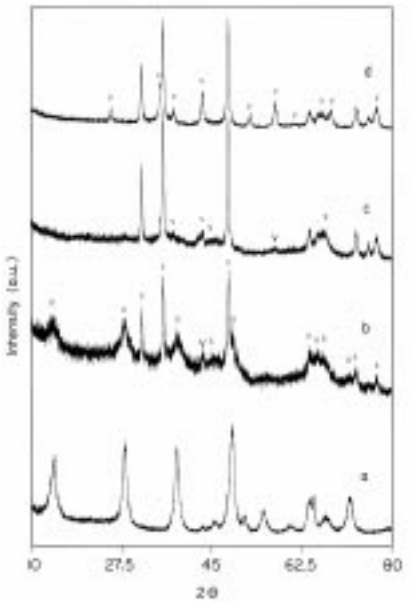

Figure 14. X-ray diffraction patterns: (a) boehmite before milling; (b) after milling the boehmite for 0.5 h (o=boehmite, v=α-Al_2O_3, s=γ-(δ-)Al_2O_3, x=WC); (c) after milling the boehmite for 1 h (v=α-Al_2O_3, s=γ-(δ-)Al_2O_3, x=WC); (d) after milling the boehmite for 2.5 h (α-Al_2O_3 and WC). The WC peaks arise due to WC contamination from the milling media.[27]

3.6. Formation of extended solid solutions

Although the transition aluminas are stable at room temperature, they are normally activated only at above-indicated temperatures. Starting from boehmite or gibsitte MG gave corundum as the final product showing the equivalence of the milling and the thermal treatment on the aluminas (Fig. 14).[27, 28] Generally it can be stated that the high-energy ball milling is a way of inducing polymorphic transformations of compounds.[8]

Generally, solid solutions are expected in binary alloys when the Hume-Rothery rules for solid solubility are satisfied (little atomic size differences, same valency, same crystal structure, little or no electronegativity difference). Serious violation of these rules was obtained using ultra-rapid quenching method,[20] and after the MA began to be used even higher extensions of supersaturated solid solutions were obtained (Table I). Even in systems where completely immiscibility in the solid and in the liquid state is known, except at very high temperatures (e.g. Al-Pb system), the supersaturated solid solution was formed by MA.[30]

Table I
Extension of equilibrium solid solubility (ESS) limits in some binary alloys on ultra-rapid quenching (URQ) from the melt and on mechanical alloying (MA)

solvent	solute	ESS (at.%)	URQ (at.%)	Ref.	MA (at.%)	Ref.
Fe	Cu	7.2	15	[20]	20	[21]
Cu	Fe	4.5	20	[20]	60	[21]
Ag	Cu	4.9	100	[20]	100	[19]
Al	Mg	18.9	36.8	[20]	40	[29]
Ni	Al	4.0			27	[31]
Ti	Mg	0.2			6	[31]
Nb	Al	10.0			30	[31]
Al	Fe	0.03	4.4	[32]	10	[31]
Al	Pb	-			1.22	[30]

3.7. Amorphization by mechanical alloying or grinding

Since P. Duwez invented the ultra rapid quenching technique, amorphous metallic phases (metallic glasses) have been produced for many years mostly by this method. However, after C. C. Koch and co-workers in 1983 synthesized an amorphous $Ni_{60}Nb_{40}$ alloy from MA of elemental Ni and Nb powders,[6] this method began to be the most utilized technique for producing amorphous materials. There were more and more experimental results available and it appeared that using the elemental powders as

starting materials in the MA process three types of amorphization reactions have been observed:[18]

type I: the characteristic feature of this type of amorphization appears is a continuous broadening of the crystalline Bragg peaks in the diffraction pattern caused by the decreasing of the crystallite size down to the nanosized values. The end product is the diffraction halo typical of amorphous materials (e.g. Ti-Cu system (Fig. 15).[22]

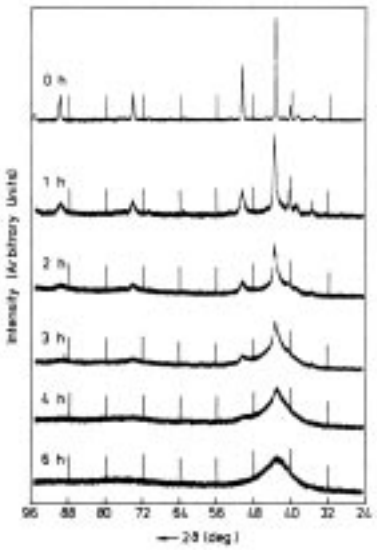

Figure 15. X-ray diffraction of $Ti_{57}Cu_{43}$ alloys. With increasing milling time, powder becomes gradually amorphous.[22]

type II: during milling the X-ray diffraction patterns show that the broad diffuse diffraction maximum of the amorphous phase grows separately, while the lines of the element powders become only slightly broader and their intensity decreases continuously during milling and finally disappears. This behavior gave evidence that the amorphization is not a continuous line broadening of the crystalline peaks, until it is impossible to distinguish between very fine microcrystallites and the amorphous phase, but a decrement of the intensity of the Bragg reflections of the elements and separately an increment of the intensity of a broad peak of the amorphous alloy. Obviously the amorphous phase grows separately as a new phase. With the aid of Sherrer formula it was found that the crystallite size reduces only to about 20 nm which is much larger than the equilibrium effective crystallite size found in type I reaction, often below 5 nm (Figs. 16 and 17).[33, 34]

type III: this reaction type is characterized by the amorphization via a crystalline

intermediate phase (e.g. Fig. 18; Nb-Sn system; reaction path: elemental powders Nb and Sn → A15 Nb_3Sn phases → amorphous phase alloys[35]).

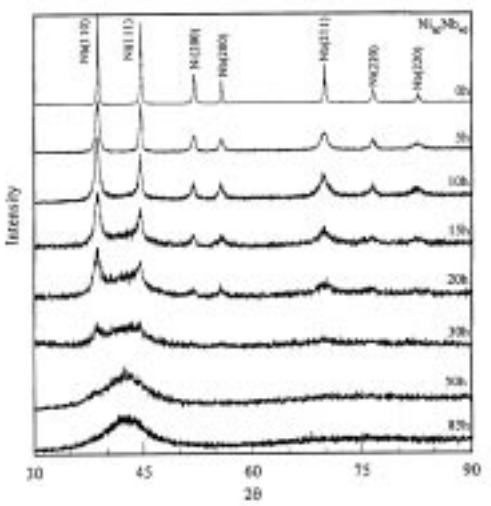

Figure 16. X-ray diffraction patterns of $Ni_{60}Nb_{40}$ powders as-received and after different milling times.[33]

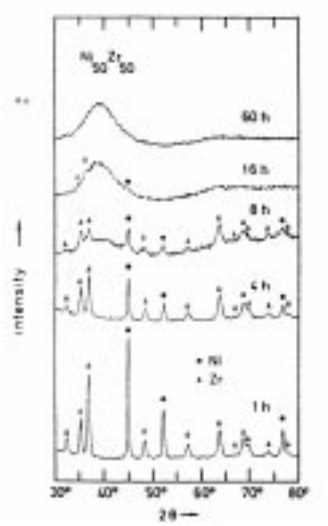

Figure 17. X-ray diffraction patterns of $Ni_{50}Zr_{50}$ powders after different milling times.[34]

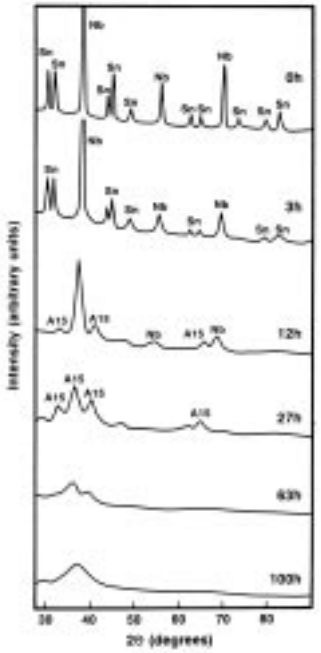

Figure 18. X-ray diffraction patterns of Nb-25at.%Sn after different milling times.[35]

At present there is no satisfactory explanation why three different types of amorphization appeared, but it exists some experimental evidence that milling equipment/conditions has/have an important influence on the type of reaction that will be observed.[18]

3.8. Temperature rise during milling

A. E. Yermakov in his paper,[5] published in 1981, attributed the amorphization reaction to a combination of fragmentation and plastic deformation produced by colliding balls, which heats local regions of the powders above their melting temperature; these melts presumably solidify sufficiently fast so as to preserve the amorphous structure. Thus the amorphous alloy would develop through a repetitive and cumulative microscopic rapid solidification process - some sort of rapidly quenching process. This explanation was practically immediately rejected but the estimation of the powder peak temperature during milling was included in many published papers. During the next 10 years numerous papers were published on this subject including theoretical calculations like the estimation of the energy flux dissipated during the shear process induced in particles trapped between two colliding balls, or experimentally like measuring the sample temperature using a thermocouple inserted into a hole in the vial side or bottom. There was a great dispersion of results: the temperature rise from about 38 K[16] to about 380 K.[25, 36]

The effective temperature present in the metallic powder during the milling is still surrounded by controversy but all agree that there is a certain temperature rise, but not more than about 300 K.[8] However, this temperature rise is quite sufficient to allow some thermal activation processes to appear and to enhance the interdifussion which showed to be one of the important factors in further models of mechanical alloying.

4. Models

4.1. Process description

Already in the first paper on mechanical alloying in 1970,[3] on observing the photomicrographs of milled powders, J. S. Benjamin noted something like layered structure and fracturation. This lead him to the conclusion that powder particles are steadily trapped between colliding balls or between ball and vial and are subjected to a severe plastic deformation, for times of the order of microseconds. Particles are repeatedly cold fractured and welded. Fracture and welding are the two basic events which produce a permanent exchange of matter between particles and ensure mixing of

the various elements of milled powders. A layered structure or lamellaes of different materials is thus formed and progressively refined (Fig. 19).[8] After longer milling a balance is achieved between welding and fragmentation which leads to a rather stable average micron or submicron particle size. However, the crystallite sizes diminish to attain a typical average size of 10 nm or lower, which means that each particle includes many nanocrystallites and a high density of grain boundaries. Finally the constituents' mixture becomes homogeneous and the elements are mixed on an atomic scale.

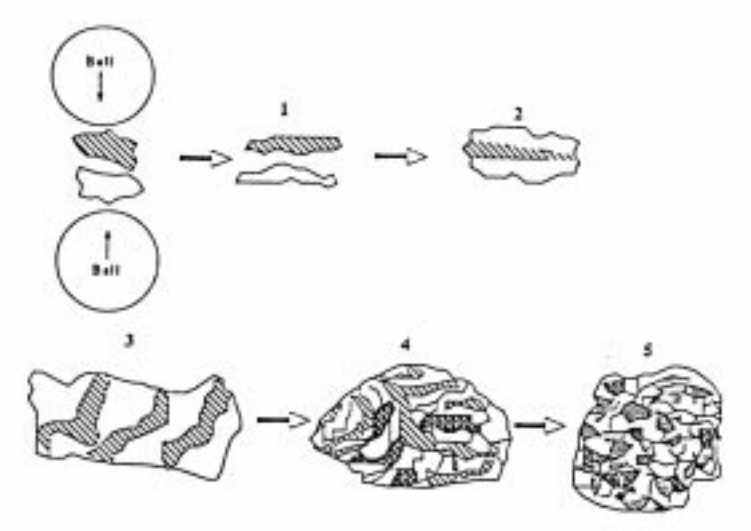

Figure 19. Stages of powder evolution during mechanical alloying of a mixture of A (white) and B (hatched) with progressive convolution of lamellae and combination of A and B).[8]

On Figs. 17 and 20(a-c) the results on Zr-Ni system, examined by X-ray diffraction (type II of amorphization), optical microscopy and scanning (SEM) are shown.[34] Optical micrographs reveal that after 0.5 h milling, the particles have a well-aligned layered microstructure (Fig. 20(a)), and the thickness of the individual layer varies from 2 to 20 μm. On SEM micrograph (Fig. 20(b)) the decrease of the average thickness of the individual layers to about 100 nm after 8 h is still clearly visible. After 16 h (Fig. 20(c)) the layered structure is no more resolvable in the scanning electron microscope. Concentration measurement still showed concentrations gradients for 35 h of milling, which disappeared after 60 hours of milling, suggesting that the material has become single phase, as seen on XRD pattern (Fig. 17). Extrapolating the layer thickness in a powder particle versus the milling time gives a layer thickness of 0.8 nm after 70 hours

of milling,[37] which represents only a few interatomic distances, confirming that the elements are mixed on the atomic scale.

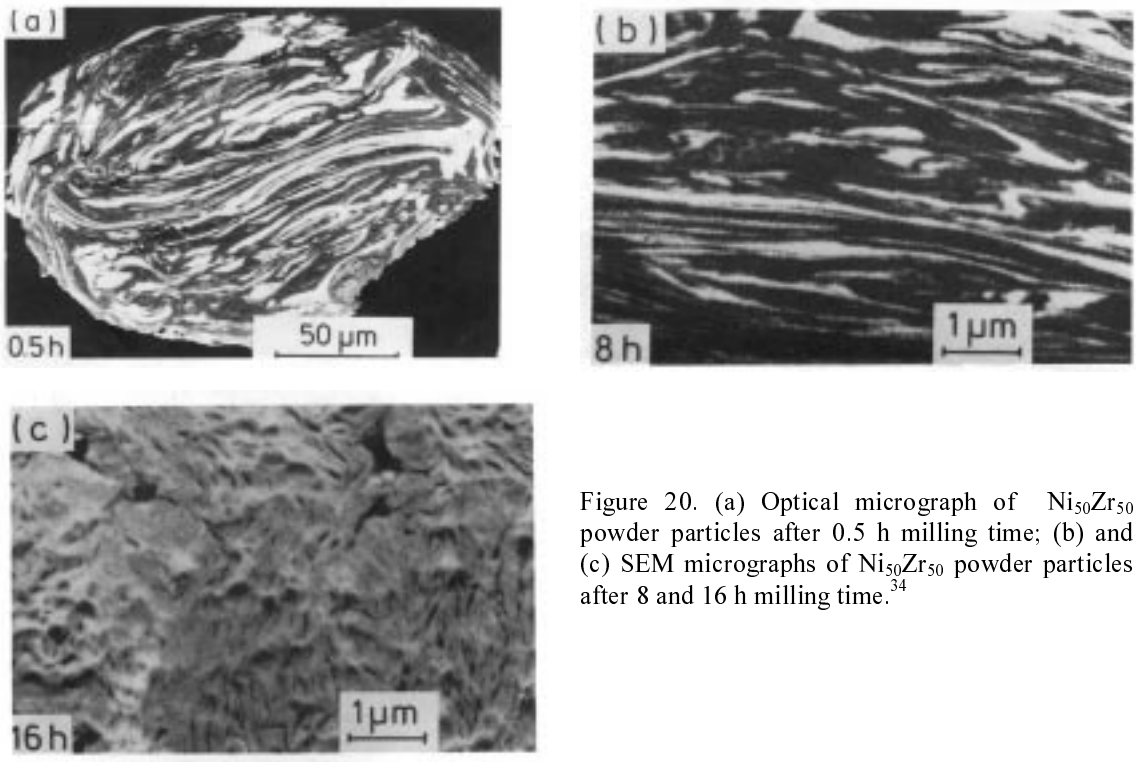

Figure 20. (a) Optical micrograph of $Ni_{50}Zr_{50}$ powder particles after 0.5 h milling time; (b) and (c) SEM micrographs of $Ni_{50}Zr_{50}$ powder particles after 8 and 16 h milling time.[34]

Even in the case of the MA of elemental Zr, Al, Cu and Ni powders to produce the quaternary $Zr_{65}Al_{7.5}Cu_{17.5}Ni_{10}$ amorphous alloy, the concentration measurements showed chemical homogeneity and the concentration of the elements was within the error limits in good agreement with the desired $Zr_{65}Al_{7.5}Cu_{17.5}Ni_{10}$ composition (an wavelength-dispersive scanning electron microscope, equipped with a microprobe quantometer (SEMQ) and a backscattering electron detector (BSE) was used).[38]

It is important to note that TEM and HTREM revealed that during the process of ball milling large deformations are introduced, like distorted regions within subgrains, grain boundaries, and even across entire grains [e.g. References 39, 40, 41]. HRTEM photographs also showed that during milling the grains slide and overlap (stacking faults and antiphase boundary are seen) and that fragmentation and adhesion of the grains is a steady process. The newly formed interfaces between grains are brought into intimate contact by subsequent ball collision forming a composite grain. Overlapping of grains is

a direct evidence that alloying takes place in layers and it was found that alloying occurs in the form of small layers having 10 nm in diameter (e.g. Figs. 6 and 21).

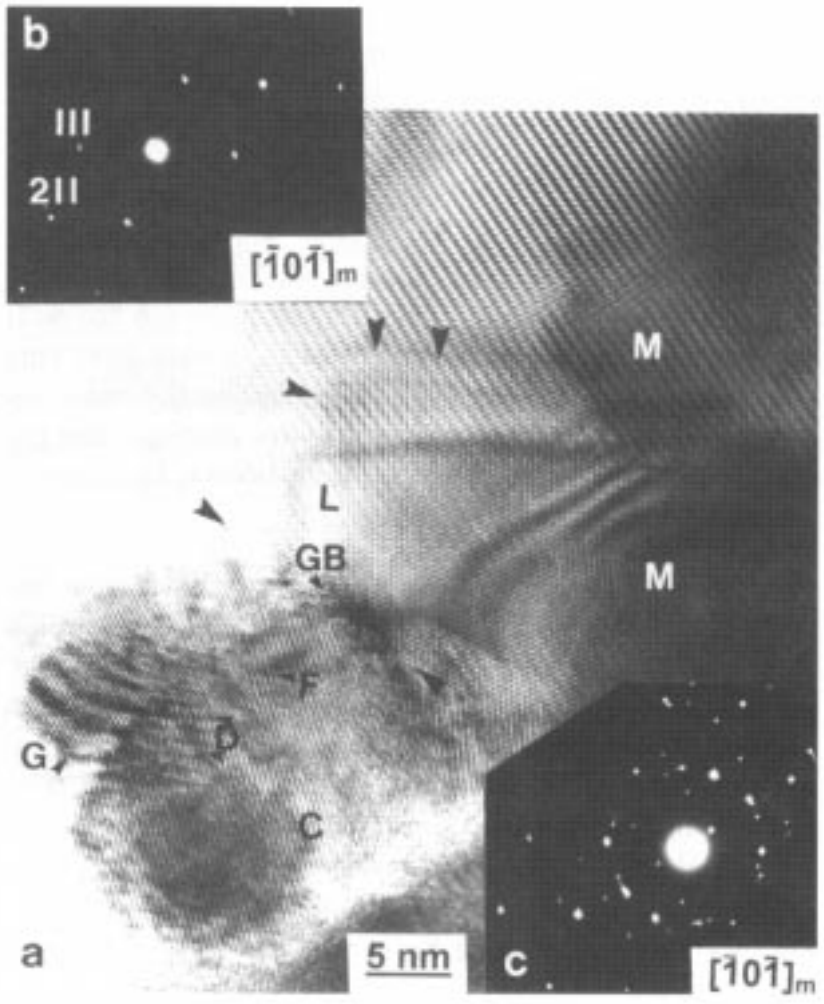

Figure 21. (a) HRTEM photograph of the mixture of *m*-ZrO_2 and Y_2O_3 powders mechanically alloyed for 10 min; (b) and (c) ED patterns of *m*-ZrO_2 and Y_2O_3.[41]

Nevertheless the reduction of layers thickness as such could not be enough to explain the complete mixing on the atomic level and some authors concluded that a dislocation kinetics which enhanced diffusitivity along the dislocation cores (dislocation pipe diffusion) is the final step for atom mixing. Namely, the MA produces fresh metal/metal surfaces and a high density of dislocations and enhances dislocation kinetics and the diffusion of solutes along dislocation cores. During successive impact, the dislocations are mechanically forced to glide, leaving behind strings of solutes in state of highly supersaturaturated state. The model can explain the formation of extended solid

solutions and amorphous alloys as well as other unusual effects observed during MA.[38, 42]

4.2. Simple thermodynamic approach

As is well known, the thermodynamic stable state of a system is determined by a minimum in the free energy, and the free energy of the equilibrium crystalline state is always lower than that of the amorphous state. It has been very early recognized that enhanced solid solubility or amorphization were first produced in systems with large negative heats of mixing, i.e.. when the lowering of the free energy of starting materials happened during the alloying process. However, on the basis of schematic diagram free energy vs composition (Fig. 22) B. Schwarz and C. C. Koch[16] first explained why thermodynamically stable phases are not formed during mechanical alloying as the end product.

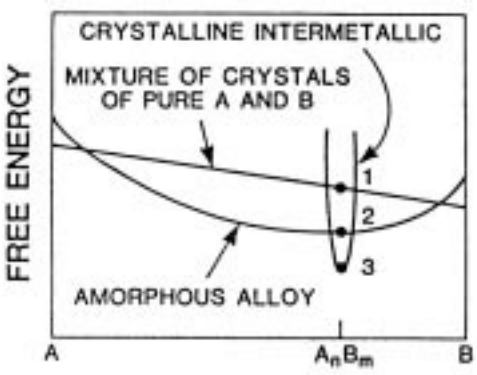

Figure 22. Schematic free energy diagram vs composition curves for a binary system AB with a negative heat of mixing in the amorphous state. (1) the mixture of pure crystalline components A and B; (2) the amorphous alloy; (3) the crystalline intermetallic compound.[16]

The straight line (1) is the free energy of a heterogeneous mixture of pure crystalline A and B powders, the broad parabola (2) is the free energy of the amorphous phase treated as an undercooled liquid with a large negative heat of mixing, and the narrow parabola (3) is the free energy of an equilibrium crystalline intermetallic compound A_nB_m. In process 1 to 2 (MA) the negative heat of mixing provides a thermodynamic driven force which favors interdiffusion leading to amorphous structure, while no such a force is present for reaction 3 to 2 (MG). However, the free energy of the crystalline phase can be raised above that of the amorphous alloy through stored energy by severe plastic deformation during milling generating point and lattice defects-vacancies, interstitials, dislocations, antiphase boundaries, etc. and induce

amorphization. Thus, when the starting product is a crystalline intermetallic one, the defect concentration must reach a critical value at which the free energy of the faulted intermetallic is above that of the amorphous phase.

However some experiments show that path 1 to 3 to 2 is also possible (Type III of amorphization (e.g. Fig. 18); elemental powders Nb and Sn → A15 Nb_3Sn phases → amorphous phase).

According to the schematic free energy diagram in Fig. 22, the free energy is first lowered from 1 to 3 forming the compound Nb_3Sn, and then it is increased to the glassy state, due to the accumulation of lattice defects.

However, if the stored energy in lattice defects or grain boundaries cannot drive the system to the amorphous state, the material will not amorphize as confirmed by the experiment for the V_3Ga compound.[43]

4.3. Systems with positive heat of mixing

Although it was recognized very early that binary systems with large negative heats of mixing of starting materials are a prerequisite for amorphization or solid solubility and that the opposite, the positive heat of mixing should not allow the amorphization or solid solubility by MA, the experiments very soon altered this opinion.

Cu and Ta are immiscible with each other even in the liquid state. However XRD patterns of 15 hours milled Cu and Ta powders show that the amorphization in a system, which possesses a positive heat of mixing, does proceed definitely by MA (Fig. 23).[44] TEM examinations support the result.[45]

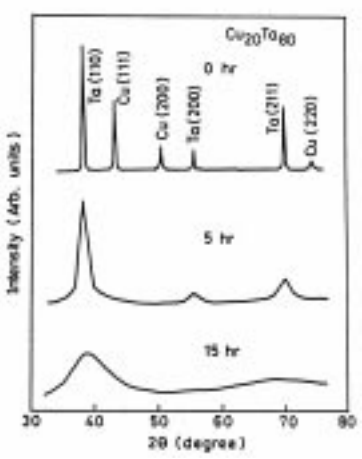

Figure 23. XRD patterns of $Cu_{20}Ta_{80}$ powders after 0, 5 and 15 h of MA.[44]

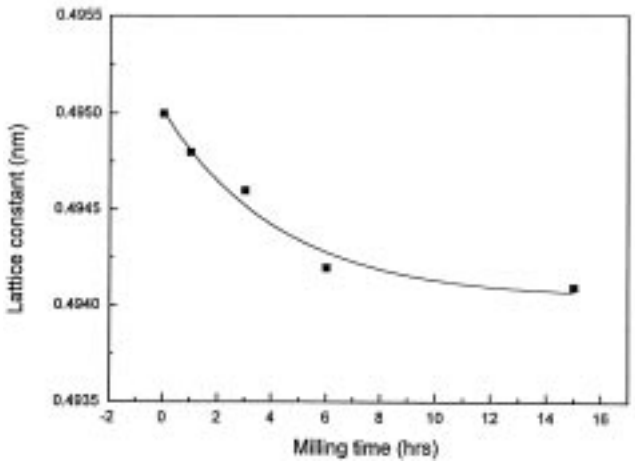

Figure 24. The dependence of lattice constant of Pb on the milling time measured in Pb-50at.%Al mechanically alloyed powder mixture.[30]

The system which is always shown as an example where both components are immiscible in both solid and liquid states (due to the positive heat of mixing) except at very high temperatures is the Pb-Al system. Unlike Ag-Cu and Fe-Cu in which supersaturated solid solutions have been obtained by both ultra-rapid quenching and MA, this is not possible in Pb-Al system by URQ. Nevertheless, it was shown during MA of elemental Pb and Al powders the Pb lattice parameter reduces slightly, which means that some Al has dissolved into the lattice of Pb (Fig. 24).[30]

All these and many other examples lead to problems because they were far from being understood from both thermodynamic and kinetics viewpoints. Several models have been proposed to explain the amorphization (e.g. very high density of defects introduced by ball milling[45]) and the mutual solubility of immiscible elements (e.g. the increment of free energy due to the large increase in the surface area caused by the formation of small fragments of components to nano-scale could provide the driving force for the formation of a supersaturated solid solution[30]) but models are still debated at present.[21, 46]

5. The influence of high-energy ball milling on science and technology

In these sections some selected examples of direct applications of MA and MG in science and technology will be presented.

MA is a process that has some advantages compared to the alloying by conventional techniques, or even by URQ. For example, alloying metals with high and low melting points by melting have drawbacks. In contrast, by using MA the problem of the different melting temperatures is overcome and so are the problems of other complicated procedures.

* $PbTiO_3$ peroviskite phase was synthesized within 20 hrs of mechanical alloying of commercial PbO and TiO_2 anatase or rutile powders. The authors claim that this is a simple, low-cost, room temperature processing technique which is free of volatility of lead.[47]

* Most of the hard intermetallic which are used as abrasive and cutting tools, like TiB_2 Ti_5Si_3 or $TiSi_2$, are all of the high melting point materials and are difficult to prepare. They are usually made in the form of thin layers using vacuum deposition techniques or in the form of powders using chemical methods. In contrast to these methods the MA technology seems to be cheaper, cleaner and more versatile than the above methods (Fig. 25).[48]

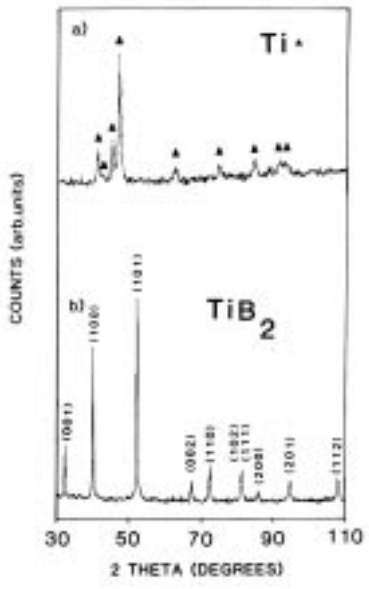

Figure 25. XRD patterns obtained from a mixture of 34at.%Ti-66at.%B mechanically alloyed for (a) 20 h and (b) 80 h; (a) peaks due to elemental titanium are marked with triangles; (b) indices due to TiB_2 are shown.[48]

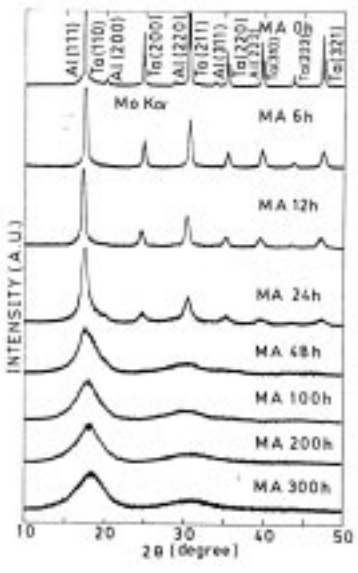

Figure 26. XRD patterns of $Al_{30}Ta_{70}$ amorphous alloy as a function of the milling time.[49]

* It is very difficult to obtain an amorphous alloy in Al-Ta system by the URQ method due to the great difference of the melting points (933 K for Al and 3293 K for Ta). However, by MA of elemental powders it was possible to produce amorphous structure in the range from 10 to 90 at.% (Fig. 26).[49]

* The conventional synthesis of the stoichiometric MnAs involves complicated melting due to the high vapor pressure of both components and the toxicity of As. These problems can be avoided using MA. After 24 hours of milling the orthorhombic MnAs phase was synthesized (Fig. 27).[50]

* Nanocrystalline magnetic materials based on FeBSi, so called FINEMET ($Fe_{73.5}Cu_1Nb_3Si_{13.5}B_9$, $Fe_{77.5}Cu_1Nb_3Si_{9.5}B_9$ or $Fe_{70}Co_{3.5}Cu_1Nb_3Si_{13.5}B_9$), present excellent soft magnetic properties mainly due to their two-phase nature with small grains embedded in a residual amorphous phase. The conventional method for preparation

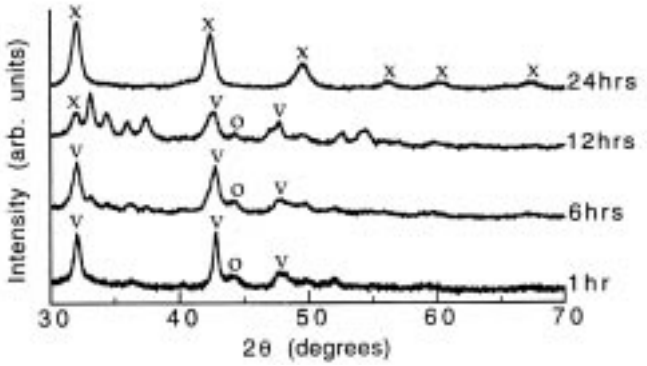

Figure 27. XRD patterns of samples milled for various times (x: MnAs; v: As; o: Mn).[50]

originates from melt spinning technology. However, by using Fe, Co, Cu, Nb, B, Si elemental powders as starting material the MA procedure was completed after 250 h of milling and the crystallite sizes were 8.6 nm. The authors of the paper compared MA samples with those obtained by melt spinning and concluded that MA is more simple and less time consuming than conventional URQ method and that the material satisfies the criteria for advance soft magnetic materials.[51]

* Yttria doped nanocrystalline zirconia powders could be prepared by rather complicated method including co-precipitation, hydrolyze and annealing at various temperatures (470 to 1670 K).[52] However by using the appropriate ratio of ZrO_2 and

Y_2O_3 oxides (or ZrO_2 with CoO, Fe_2O_3 and α–Al_2O_3) the alloying in a high-energy ball mill is completed within 3 hours (Figs. 29-30).[12]

* It was found[53] that MA of CuO and ZnO with Ca resulted in the formation of Cu and Zn respectively (CuO+Ca → Cu+CaO; ZnO+Ca → Zn +CaO). Also the MA of CuO and ZnO together with Ca resulted in the formation β'brass (CuO+ZnO+Ca → β'brass+CaO). The process may find application in the production of reactive elements and alloys, such as the rare earth, which are difficult to produce using conventional metallurgical processing (temperatures over 1400 K are needed).

* One of the problems in the development of hydrogen related technologies (i.e. hydrogen fueled vehicles) is the hydrogen storage and one of the existing competing technology is based on metal hydrides, like MgH_2, which seems to be the safest of all, but there is the problem of low capacity storage, to high absorption (≈ 470 K) and

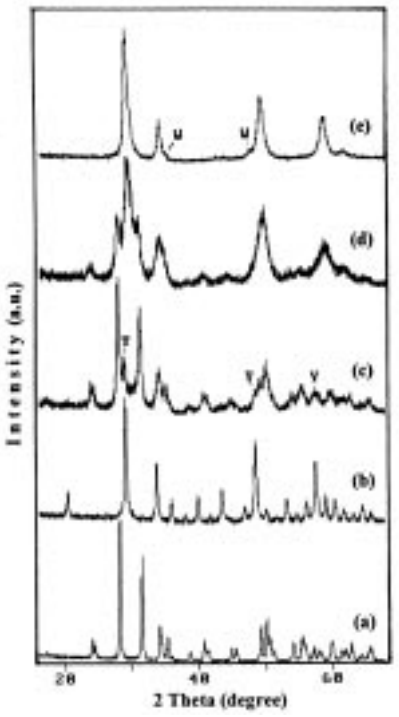

Figure 29. XRD patterns of: (a) monoclinic ZrO_2: (b) cubic Y_2O_3; (c) mixture of 2.5 g ZrO_2 and 0.5 g Y_2O_3 powder MA for 10 min; (d) mixture of 2.5 g ZrO_2 and 0.5 g Y_2O_3 powder MA for 60 min; (e) mixture of 2.5 g ZrO_2 and 0.5 g Y_2O_3 powder MA for 180 min. Symbols are as follows: Y: Y_2O_3; W: WC.[12]

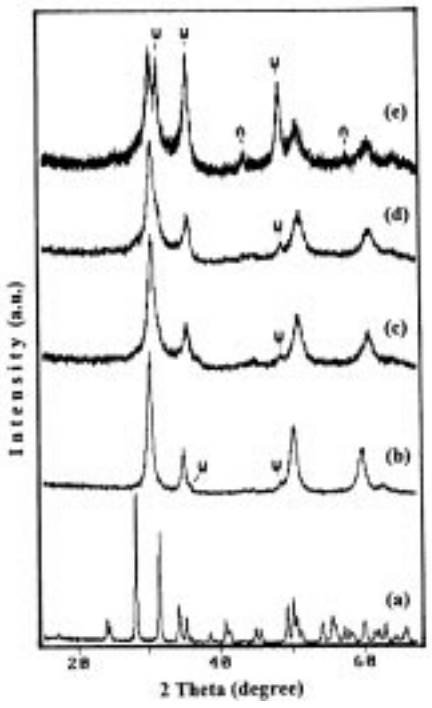

Figure 30. XRD patterns of: (a) monoclinic ZrO_2: (b) mixture of 2.5 g ZrO_2 and 0.5 g Y_2O_3 powder MA for 180 min; (c) mixture of 2.5 g ZrO_2 and 0.5 g CoO powder MA for 180 min.; (d) mixture of 2.5 g ZrO_2 and 0.5 g Fe_2O_3 powder MA for 180 min; (e) mixture of 2.5 g ZrO_2 and 0.5 g α-Al_2O_3 powder MA for 180 min. Symbols are as follows: A: α-Al_2O_3; W: WC.[12]

desorption (>670 K) temperature. However, ball milling of MgH_2 phase induces drastic changes in the structure of the material (reduction of the crystal size which increases the effective surface area of powder from 1.2 to 9.9 m^2g^{-1}, i.e. by the factor of about ten in comparison to conventional preparation techniques, appearance of a new phase, introduction of the structural defects). Measurements show a drastic improvement in the hydrogen absorption and desorption showing that the MG cause is a good step in the direction of developing practical high storage capacity metal hydrides for vehicular applications.[54]

* Copper indium diselenide ($CuInSe_2$)-based photovoltaic solar cells have received considerable attention in recent years because of their high conversion efficiency. They are usually obtained by either multisource thermal evaporation and co-deposition or reactive annealing of precursor films. These processes are very involved, contain a number of deposition and annealing steps, and can be expensive. But on milling for only 20 minutes of the mixture of elemental powders of copper and selenium and fine chips/granules of gallium and indium in corresponding weights a homogeneous 8 nanometer sized nanocrystalline $CuIn_{0.7}Ga_{0.3}Se_2$ alloy was synthesized.[55]

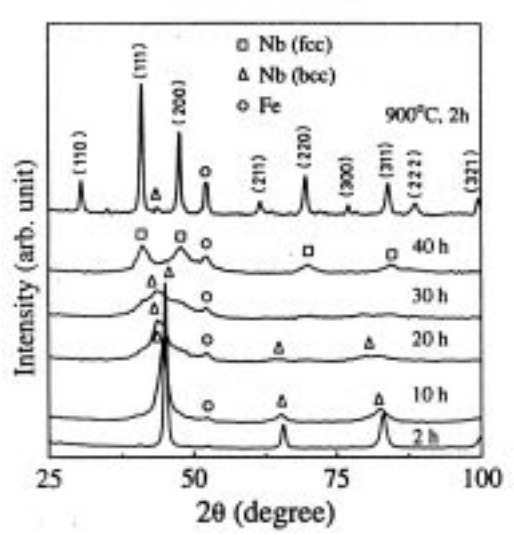

Figure 31. XRD patterns of ball milled $Nb_{80}Al_{20}$ samples at different times. The peaks with symbol (o) arise due to α-Fe contamination from the chrome steel milling media.[55]

At the end of this chapter we should mention the greatest problem, which appears during MA or MG procedure. Let us look at only two examples (Fig. 30 and Fig. 31), where it can be seen that a very high level of contamination could be introduced into materials by mechanical milling. The most important source of contamination is the erosion (wear) of the balls and of the container during the milling process, as well as oxidation or reaction with nitrogen or hydrogen which cannot be avoided when milled in these atmospheres. At the present state the contamination cannot be avoided, but only minimized.

6. **Conclusions**

1) Mechanical alloying (MA) is a high-energy ball milling process employed to synthesize a variety of stable and metastable nanosized highly homogenized materials, including supersaturated solid solutions, intermetallics, amorphous alloys, and also a variety of technologically useful materials, which are very difficult to manufacture by other techniques, like alloying of elements with high and low melting points.

2) Mechanical alloying is a simple, quick, cheap and easily controllable alloying technique.

3) There are practically no limits (restrictions) on materials which could be alloyed/synthesized by MA.

4) By milling it is possible to produce a large quantity of powder, which might be used to obtain bulk material for further studies of physical properties. This is in contrast to the materials obtained by traditional ultra rapid quenching, whereby only thin ribbons or thin films are obtained.

5) MA could induce amorphization (and metastable solid solubility also) in systems which could not be amorphized by other nonequilibrium processes like very rapid quenching. As a consequence it offers the possibility to design new alloys, which cannot be produced by URQ.

6) The contamination of the end products is a serious problem and “clean” milling is expected in the future.

7. References

[1] P. Duwez, *Transaction of the ASM* **1960**, *60*, 607-633.
[2] R. W. Cahn, A. L. Greer, Metastable States of Alloys, in *Physical Metallurgy;* Editors: R. W. Cahn, P. Haasen, North-Holland, Amsterdam, 1996, pp 1724-1830.
[3] J. S. Benjamin, *Metall. Trans.* **1970**, *1*, 2943-2951.
[4] R. L. White, Ph. D. dissertation, Stanford University, 1979.
[5] A. E. Yermakov, E. E. Yurchikov, V. A. Barinov, *Fiz. Metal. Metalloved.* **1981**, *52*, 1184-1193.
[6] C. C. Koch, O. B. Cavin, C. G. McKamey, I. O. Scabrough, *Appl. Phys. Lett.* **1983**, *43*, 1017-1019.
[7] R. B. Schwarz, R. R. Petrich, C. K. Saw, *J. Non-Cryst. Solids* **1985**, *76*, 281-302.
[8] E. Gaffet, F. Bernard, J. Niepce, F. Charlot, C. Gras, G. Le Caër, J. Guichard, P. Delcroix, A. Mocellin, O. Tillement, *J. Mater. Chem.* **1999**, *9*, 305-314.
[9] R. R. Soni, *Mechanical Alloying-Fundamentals and Application*; Cambridge Inter. Sci. Pub., Cambridge, 2000.
[10] J. Eckert, J. C. Holzer, C. E. Krill, W. L. Johnson , *J. Mater. Res.* **1992**, *7*,1980-1983.
[11] J. Eckert, J. C. Holzer, C. E. Krill, W. L. Johnson , *J. Mater. Res.* **1992**, *7*, 1751-1761.
[12] A. M. Tonejc, A. Tonejc, *Mater. Sci. Forum* **1996**, *225*-227, 497-502.
[13] H. Gleiter, Microstructure, in *Physical Metallurgy;* Editors: R. W. Cahn, P. Haasen, North-Holland, Amsterdam, **1996**, pp 844-942.
[14] X. Zhu, R. Biringer, U. Herr, H. Gleiter, *Phys. Rev. B* **1987**, *35*, 9085-9090.
[15] K. Lu, Y. Zhao, *NanoStructured Mater.* **1999**, *12*, 559-562.
[16] R. B. Schwarz and C. C. Koch, *Appl. Phys. Lett.* **1986**, *49*, 146-148.
[17] A. W. Weeber, H. Bakker and F. R. de Boer, *Europhys. Lett.* **1986**, *2*, 445-448.
[18] A. W. Weeber, H. Bakker, *Physica B* **1988**, *153*, 93-135.
[19] K. Uenishi, K. F. Kobayashi, K. N. Ishihara, P. H. Shingu, *Mat. Sc. Engng. A* **1991**, *134*, 1342-1345.
[20] T. R. Anantharaman, C. Suryanarayana, *J. Mater. Sci.* **1971**, *6*, 1111-1135.
[21] Y. Yang, Y. Zhu, Q. LI, X. Ma, Y. Dong, G. Wang, S. Wei, *Physica B* **2001**, *293*, 249-259.
[22] C. Politis, W. L. Johnson, *J. Appl. Phys.* **1986**, *60*, 1147-1151.
[23] J. Chitralekha, K. Raviprasad, E. S. R. Gopal, K. Chattopadhyay, *J. Mater. Res.* **1995**, *10*, 1897-1904.
[24] A. Inoue, H. M. Kimura, K. Matsuki, T. Masumoto, *J. Mat. Sci. Lett.* **1987**, *6*, 979-981.
[25] L. Schultz, *J. Less-Common Metals* **1988**, *145*, 233-249.
[26] L. Schultz. *Mat. Sci. Engng.* **1988**, *97*, 15-23.
[27] A.Tonejc, C. Kosanović, A. M. Tonejc, M. Stubičar, B.Subotić, I. Šmit, *J. All. Comp.* **1994**,*204*, L1-L3.
[28] A.Tonejc, A. M. Tonejc and D. Bagović, *Mater. Sci. Engng.* **1994**, *A181/A182*, 1227-1231.
[29] A. Calka, W. Kaczmarek, J. S. Williams, *J. Mater. Sci.* **1993**, *28*, 15-18.
[30] M. Zhu, Z. Che, Z. X. Li, J. K. L. Lai, M. Qi, *J. Mater. Sci.* **1998**, *33*, 5873-5881.
[31] C. C. Koch, *Mater. Sci. Forum,* **1992**, *88-90*, 243-262.
[32] A. Tonejc, A. Bonefačić, *J. Appl. Phys.* **1969**, *40*, 419-420.
[33] P. Schumacher, M. H. Enayati, B. Cantor, *J. Metast. and Nanocryst. Mater.* **1999**, *2-6*, 351-356.
[34] Eckert, L. Schultz, K. Urban, *J. Non-Cryst. Solids* **1991**, *130*, 273-286.
[35] M. S. Kim and C.C. Koch, *J. Appl. Phys.* **1987**, *61*, 3450-3453.
[36] J. S. Benjamin, *Mater. Sci. Forum,* **1992**, *88-90*, 1-18.
[37] A. W. Weeber, H. Bakker, H.J.M. Heijligus, G.F. Bastin, *Europhys. Lett.* **1987**, *3*, 1261-1265.
[38] M. Seidel, J. Eckert, I. Bächer, M. Reibold, L. Schultz, *Acta. Mater.* **2000**, *48*, 3657-3670.
[39] A. M. Tonejc, A. Tonejc, G. W. Farrants, S. Hovmöller, *Cro. Chem. Acta* **1999**, *72*, 311-326.
[40] T. Chen, J. M. Hampikian, N. N. Thadhani, *Acta Mater.* **1999**, *47*, 2567-2579.
[41] A. M. Tonejc, *Acta Chim. Slov.* **1999**, *46*, 435-461.
[42] R. B. Schwarz, *Mater. Sci. Forum* **1998**, *269-272*, 665-674.

[43] L. M. Di, H. Bakker, *J. Phys.: Condens. Matter.* **1991**, *3*, 3427-3432.
[44] T. Fukunaga, K. Nakamura, K. Suzuki, U. Mizutani, *J. Non-Cryst. Solids* **1990**, *117/118*, 700-703.
[45] L. Liu, Z. Q. Chu and Y. D. Dong, *J. All. Comp.* **1992**, *186*, 217-221.
[46] J. Xu, G. S. Collins, L. S. J. Peng, M. Atzmon, *Acta Mater*. **1999**, *47*, 1241-1253.
[47] L. Kong, W. Zhu, O. K. Tan, *Ferroelectrics* **1999**, *230*, 281-286.
[48] A. P. Radlinski, A. Calka, *Mat. Sc. Engng. A* **1991,** *134*, 1376-1379.
[49] M.S.El-Esksndarany, F. Itoh, K. Aoki, K. Suzuki, *J. Non-Cryst. Solids* **1990**, *117/118*, 729-732.
[50] L. Wee, P.G. McCormick and R. Street, *Scripta Materialia* **1999**, *40*, 1205-1208.
[51] H. Chiriac, A.E.Moga, M. Urse, F. Necula, *NanoStructured Materials* **1999**, *12*, 495-298.
[52] R. Ramamoorthy, S. Ramasamy, *J. Mater. Res*. **1999**, *14*, 90-96.
[53] G. B. Schaffer, P. G. McCormick, *Appl. Phys. Lett.* **1989**, *555*, 45-46.
[54] A. Zaluska, L. Zaluski, J. O Ström-Olsen, *J. All. Comp*. **1999**, *289*, 197-206.
[55] C. Surynarayana, E. Ivanov, R. Noufi, M. A. Contreras, J.J. Moore, *J. Mater. Res.* **1999**, *14*, 377-383.
[56] P. P. Chatterjee, S. K. Pabi, I. Manna, *J. Appl. Phys*. **1999**, *86*, 5912-5914.

Povzetek

Mletje v visokoenergijskih krogličnih mlinih, v katerih poteka zlivanje(MA) in mletje(MG) se v zadnjih dveh desetletjih široko uporablja kot alternativa kristalizaciji z ultra hitrim hlajenjem za pripravo raznih vrst materialov. Pri mehanskem zlivanju različnih prašnatih materialov kakor tudi pri mletju snovi enake sestave v omenjenih mlinih dobimo široko paleto popolnoma novih metastabilnih zlitin.

Velikost delcev hitro pada s časom mletja do končnega produkta, zlitin nanomaterialov velikosti 1 – 30 nm. Med mletjem lahko interakcije med mlevnimi kroglami in prašnimi delci opišemo kot hladno spajkanje, plastično deformiranje in drobljenje. Pri tem so za spremembo strukture potrebne nizke aktivacijske energije.

V prispevku je podana termodinamska in kinetična razlaga mehnizma nastajanja metastabilne faze med mletjem v sistemih, ki izkazujejo negativno toploto mešanja komponent. Prikazana je tudi možna razlaga nastajanja metastabilne faze v sistemih s pozitivno toploto mešanja. Orisana so tudi različna možna področja uporabe obravnavane tehnologije.